

# The dependence of terahertz radiation on the built-in electric field in semiconductor microstructures

Jenn-Shyong Hwang<sup>\*1</sup>, Hui-Ching Lin<sup>1</sup>, Chin-Kuo Chang<sup>1</sup>, Tai-Shen Wang<sup>1</sup>, Liang-Son Chang<sup>1</sup>, Jen-Inn Chyi<sup>2</sup>, Wei-Sheng Liu<sup>2</sup>, Shu-Han Chen<sup>2</sup>, Hao-Hsiung Lin<sup>3</sup>, and Po-Wei Liu<sup>3</sup>

<sup>1</sup> Dept. of Physics, National Cheng Kung University, 1 Ta-Hsueh Road, Tainan, Taiwan 70101;

<sup>2</sup> Dept. of Electrical Engineering, National Central University, Chung-Li, Taiwan;

<sup>3</sup> Dept. of Electrical Engineering, National Taiwan University, Taipei, Taiwan

[pjshwang@mail.ncku.edu.tw](mailto:pjshwang@mail.ncku.edu.tw)

**Abstract:** The amplitudes of terahertz radiation are measured for a series of GaAs surface intrinsic-n<sup>+</sup> structures with various built-in surface electric fields as the bias. As the surface field is lower than the so-called “critical electric field” related with the energy difference between the  $\Gamma$  to L valley of the semiconductor, the amplitude is proportional to the product of the surface field and the number of photo-excited carriers. As the surface field exceeds the critical field, the amplitude is independent of the surface field but proportional to the product of the critical field and the number of the photo-excited carriers.

©2007 Optical Society of America

**OCIS codes:** (320.7130) Ultrafast processes in condensed matter, including semiconductor; (300.6470) Spectroscopy, semiconductors; (160.6000) Semiconductors, including MQW.

---

## References and links

1. P. Gu, M. Tani, S. Kono, and K. Sakai, “Study of terahertz radiation from InAs and InSb,” *J. Appl. Phys.* **91**, 5533-5537 (2002).
2. S. Winnerl, S. Sinning, T. Dekorsy, and M. Helm, “Increased terahertz emission from thermally treated GaSb,” *Appl. Phys. Lett.* **85**, 3092-3094 (2004).
3. L. Xu, X. C. Zhang, and D. H. Auston, “Terahertz radiation from large aperture Si p-i-n diodes,” *Appl. Phys. Lett.* **59**, 3357-3359 (1991).
4. H. Shen, M. Dutta, L. Fotiadis, P. G. Newman, R. Moerkirk, W. H. Chang, and R. N. Sacks, “Photoreflectance study of surface Fermi level in GaAs and GaAlAs,” *Appl. Phys. Lett.* **57**, 2118-2120 (1990).
5. H. Shen, M. Dutta, R. Lux, W. Buchwald, and L. Fotiadis, “Dynamics of photoreflectance from undoped GaAs,” *Appl. Phys. Lett.* **59**, 321-323 (1991).
6. X. Yin, H. M. Chen, F. H. Pollak, Y. Chen, P. A. Montano, P. D. Kirchner, G. D. Pettit, and J. M. Woodall, “Photoreflectance study of surface photovoltage effects at (100)GaAs surfaces/interfaces,” *Appl. Phys. Lett.* **58**, 260-262 (1991).
7. J. S. Hwang, W. C. Hwang, Z. P. Yang, and G. S. Chang, “Energy spectrum of surface states of lattice-matched In<sub>0.52</sub>Al<sub>0.48</sub>As surface intrinsic-n<sup>+</sup> structure,” *Appl. Phys. Lett.* **75**, 2467-2469 (1999).
8. J. S. Hwang, K. I. Lin, H. C. Lin, S. H. Hsu, K. C. Chen, Y. T. Lu, Y. G. Hong, and C. W. Tu, “Studies of band alignment and two-dimensional electron gas in InGaPn/GaAs heterostructures,” *Appl. Phys. Lett.* **86**, 061103 (2005).
9. J. N. Heyman, N. Coates, and A. Reinhardt, “Diffusion and drift in terahertz emission at GaAs surfaces,” *Appl. Phys. Lett.* **83**, 5476-5478 (2003).
10. X. C. Zhang, and D. H. Auston, “Optoelectronic measurement of semiconductor surfaces and interfaces with femtosecond optics,” *J. Appl. Phys.* **71**, 326-338 (1992).
11. Y. Cai, I. Brener, J. Lopata, J. Wynn, L. Pfeiffer, and J. B. Stark, “Coherent terahertz radiation detection: Direct comparison between free-space electro-optic sampling and antenna detection,” *Appl. Phys. Lett.* **73**, 444-446 (1998).
12. J. R. Hook and H. E. Hall, *Solid State Physics* (John Wiley & Sons, 1991), Chap. 5.
13. A. Leitenstorfer, S. Hunsche, J. Shah, M. C. Nuss, and W. H. Knox, “Detectors and sources for ultrabroadband electro-optic sampling: Experiment and theory,” *Appl. Phys. Lett.* **74**, 1516-1518 (1999).
14. A. Leitenstorfer, S. Hunsche, J. Shah, M. C. Nuss, and W. H. Knox, “Femtosecond charge transport in Polar Semiconductors,” *Phys. Rev. Lett.* **82**, 5140-5143 (1999).

## 1. Introduction

Free-space pulsed terahertz (THz) radiation can be generated by the motion of photo-excited electrons and holes that are accelerated by the local or bias field which may be an external applied field or an internal field in charge depletion layers resulting from the charge transfer due to a Schottky contact and a p-n junction, etc.[1-3]. The amplitude of the THz radiation is widely believed to be proportional the local or bias field,  $E_{loc}$ , as well as the number of photo-excited carriers  $n_{ph}$ . In this study, the amplitudes of the THz radiation are measured for a series of GaAs surface intrinsic-n<sup>+</sup> (SIN<sup>+</sup>) structures with various built-in surface fields. It is found that as the surface field in the intrinsic layer is lower than the so-called "critical electric field,  $E_c$ " of the semiconductor, the amplitude of the THz radiation depends not only on the strength of the surface field but also the number of photo-excited carriers. At the high field limit, on the other hand, at which the surface field exceeds the critical electric field, the THz amplitude is independent of the surface field but proportional to the number of photo-excited carriers.

## 2. Experimental results and discussions

GaAs SIN<sup>+</sup> structures [4-6] grown by conventional molecular beam epitaxy (MBE) are used as the THz emitters in this study. These as-grown hetero-structures possess a common structure consisting of 800, 600, 400, 200, 100, and 50nm undoped GaAs layer (intrinsic layer) grown on top of 1 $\mu$ m n-type GaAs buffer layer, with doping concentration around  $1 \times 10^{18} \text{ cm}^{-3}$ , which are grown previously on SI (100) GaAs substrate. Both the buffer and intrinsic layer share the same direction along (100) with the substrate. A built-in static electric field exists across the intrinsic layer similar to a parallel-plate capacitor with electrons accumulated at the surface and ionized positive donors behind the interface. Various intrinsic layer (undoped layer) thicknesses are also obtained from as-grown samples by subsequent etches. The surface fields in these samples measured by modulation spectroscopy of photorefectance (PR) ranges from 14 to 297 KV/cm, a range which brackets the critical electric field [7-8].

PR measurements, as described previously [7-8], are taken at room temperature. A standard arrangement of the PR apparatus is used in this study. The probe beam consists of a Xe-Arc lamp and a quarter-meter monochromator combination. A He-Ne laser served as the pumping beam. The detection scheme consists of a Si photo-detector and a lock-in amplifier. The modulated reflectance signals ( $\Delta R/R$ ) are processed by the lock-in amplifier and a PC computer. For a detailed description of the PR spectroscopy apparatus, the reader is referred to the references [7-8]. Figure 1 displays the PR spectra from all the as-grown samples. Features near 1.3-1.4 eV originate from the GaAs substrate, while features from 1.5-1.8 eV were the Franz-Keldysh oscillations, (FKO, labeled 1-9 in Fig. 1) originating from the built-in electric field in the undoped layer. The photon energy  $E_n$  of the  $n_{th}$  extremum of the FKO plotted as a function of  $F_n$ , defined by  $[3\pi(n+1/2)/2]^{2/3}$ , yields a straight line. From the slope of this straight line and the formula in Ref. [8], the built-in electric field and energy gap  $E_g$  of the sample can be deduced. The FKO extrema  $E_n$  plotted as a function of  $F_n$  for the GaAs sample with different undoped layer thickness is shown in Fig. 2. The energy gap obtained is 1.42 eV for all samples and is independent of the undoped layer thickness  $d$ . Figure 3 displays the built-in electric fields of all the samples as a function of  $d$ . Data obtained from samples successively etched from as-grown samples with undoped layer of 800 nm, are shown in solid squares. Whether achieved through etching or as-grown, samples with identical undoped layer thickness have similar built-in electric field, implying that undoped layer thickness is correctly measured in the etching process. The built-in electric fields from

samples in which the undoped layer is completely etched away or all the way through to the buffer layer are also included in Fig. 3. The negative values of  $d$  represent the thickness of the buffer layer that is etched away. While the undoped layer is completely removed, or the buffer layer is partially etched away, the measured electric field locates in the charge depletion layer of the buffer.

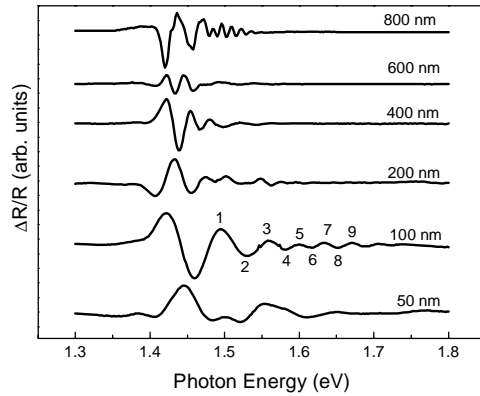


Fig. 1. The PR spectra from all the as-grown samples.

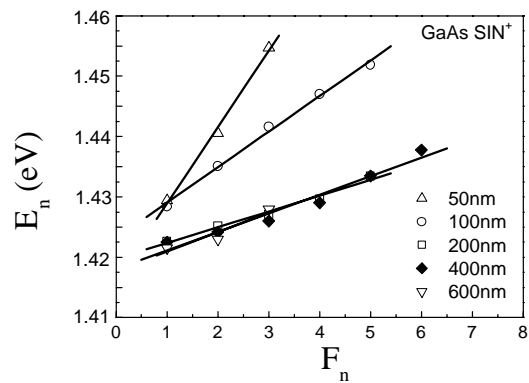


Fig. 2. The FKO extrema  $E_n$  plotted as a function of  $F_n$  for the GaAs sample with different undoped layer thickness

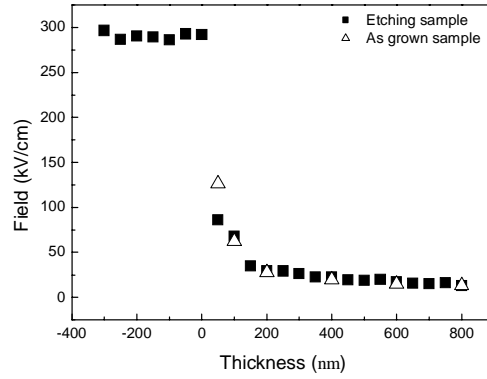


Fig. 3. The built-in electric fields of all the samples as a function of intrinsic layer thickness  $d$ .

A standard experiment setup using a free-space co-propagating electro-optic sampling system is employed. THz radiation is detected in reflection geometry. A mode-locked Ti:Sapphire laser operated at 82 MHz is used to generate 80 fs pulses with a central wavelength of around 790 nm. The incident angle of the pump laser on the sample is  $45^\circ$  from normal. The pump beam is uniformly focused on the emitter surface in s-polarization and maintained at 200 mW over an area with radius of  $500\mu\text{m}$ . Since the pump beam intensity is low (around  $0.3\mu\text{ J/cm}^2$ ) and the emitter possesses inversion symmetry, there is little contribution from nonlinear process. The THz radiation is collected by a pair of parabolic mirrors and focused on a 2 mm thick ZnTe crystal. Figure 4 depicts the amplitude of the THz radiation from the GaAs  $\text{SIN}^+$  structure as a function of the thickness of the intrinsic layer. The inset displays several time domain THz spectra of samples with different intrinsic layer thicknesses.

The amplitude of THz radiation is proportional to volume integral of the time derivative of the transient current density  $J(x,t)$ , which equals  $e n_{\text{ph}}(x,t) \mu E_{\text{loc}}$ , where  $n_{\text{ph}}(x,t)$  is the density of photo-excited carriers,  $e$  is the electron charge,  $\mu$  is the electron mobility and  $E_{\text{loc}}$  is the electric field. Here we have neglect the contribution from diffusion of electrons due to  $k_B T \ll eE/\alpha$  in our case [9]. By neglecting the change of electron of mobility related to the relaxation of hot electron energy which is in a time scale much larger than the excitation of photo-carriers, and neglecting the change of electric field due to the photo-generated carrier screening effect, we obtain [9-12]

$$\frac{\partial J(x,t)}{\partial t} \propto e E_{\text{loc}} \mu \frac{\partial n_{\text{ph}}(x,t)}{\partial t} \quad (1)$$

Integrating over the volume of the excitation, we obtain the amplitude of the THz radiation as

$$E_{\text{THz}} \propto n_{\text{ph}} \mu E_{\text{loc}} \quad (2)$$

where  $n_{\text{ph}}$  is the total number of photo-excited carriers in the depletion and surface-intrinsic layers per excitation pulse

$$n_{\text{ph}} = \frac{\eta(1-R)}{\hbar\omega \cos\theta_n} \int_0^{d+s} I_0 \exp(-\alpha x / \cos\theta_n) \alpha dx \quad (3)$$

with  $R$  the reflectivity of the emitter,  $\alpha$  the absorption coefficient ( $1.40 \times 10^4 \text{ cm}^{-1}$  for GaAs),  $\eta$  the quantum efficiency,  $\hbar\omega$  the photon energy of the pump beam,  $\gamma$  the repetition rate of the

pump beam (82 MHz here),  $\theta_n$  the angle that the intrinsic layer optical path makes with the surface normal (x-direction),  $d$  the thickness of the intrinsic layer in the  $\text{SIN}^+$  structure used as an emitter, and  $s$  the width of the charge depletion layer defined by  $s = \sqrt{\frac{2\epsilon_0\epsilon_r\phi}{eN}}$  where  $\epsilon_r$  is the dielectric constant of the semiconductor,  $N$  is the doping concentration, and  $\phi$  is the potential barrier height across the interface or the charge depletion layer on the surface. In the experiment reported herein,  $I_0$  is maintained at 200mW over an area with radius of 500 $\mu\text{m}$ . The number of photo-excited free carriers  $n_{\text{ph}}$  are estimated by Eq. (3). The THz radiation and the product,  $n_{\text{ph}}E_{\text{loc}}$ , are plotted in solid squares and open circles, respectively, as a function of the thickness of the intrinsic layer, in Fig. 5.

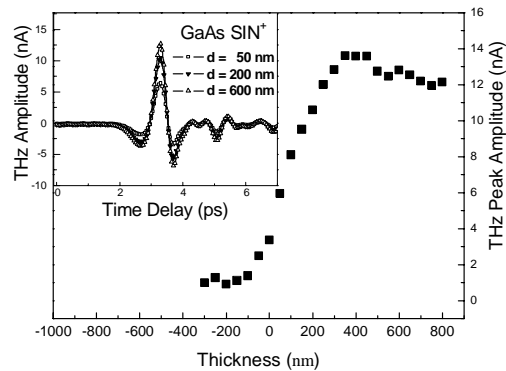


Fig. 4. The amplitude of the THz radiation from the GaAs  $\text{SIN}^+$  structures with various intrinsic layer thickness. The inset displays several time domain THz spectra of samples with different intrinsic layer thicknesses.

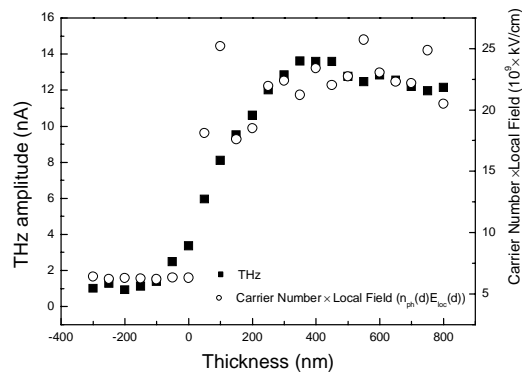


Fig. 5. The THz radiation and the product of  $n_{\text{ph}}E_{\text{loc}}$ , plotted in solid squares and open circles, respectively, as a function of the thickness of the intrinsic layer.

Figures 3 and 5, however, reveal that the variations of the amplitude of the THz radiation and the product,  $n_{\text{ph}}E_{\text{loc}}$ , are not consistently related to each other when the thickness of the intrinsic layer is less than 200 nm or the built-in electric fields in the emitters is larger than 40 KV/cm. Leitenstorfer et al.[13-15] found that, below the so-called critical electric field, the

maximum drift velocity of free charged carriers in a semiconductor is proportional to the electric field in the semiconductor. However, as the field rises above the critical electric field,  $E_c$ , the maximum drift velocity declines slightly as the field increases. The maximum drift velocity of the free charged carriers peaks at the critical electric field, which depends on the energy difference between the  $\Gamma$  to L valley (intervalley threshold, L valley offset) in the semiconductor. Leitenstorfer et al. also found that the critical electric field in GaAs is 40 KV/cm corresponding to an intervalley threshold of 330 meV. Figure 3 indicates that while the intrinsic layer thickness is less than 200 nm, the electric field of GaAs is larger than the critical field thus the drift velocity is approximately constant. The amplitude of THz radiation, above the so-called critical electric field, is not proportional to  $n_{ph}E_{loc}$  but proportional to  $n_{ph}E_c$ . We can define an effective electric field,  $E_{eff}$ , which equals to the critical field,  $E_c$  as the  $E_{loc}$  is larger than the critical field, and equals to  $E_{loc}$  as the  $E_{loc}$  is smaller than the critical field. Figure 6 plots  $n_{ph}E_{eff}$  as a function of the intrinsic layer thickness ( $d$ ). For comparison, the amplitude of the THz is also plotted as a function of  $d$  in Fig. 6. The dependence of THz and  $n_{ph}E_{eff}$  on the thickness of the intrinsic layer are almost identical to each other implying that there is a critical electric field,  $E_c$ , in the semiconductor such that  $E_{THz}$  is dependent on  $E_{loc}$  when  $E_{loc}$  is smaller than  $E_c$  and is independent of  $E_{loc}$  when  $E_{loc}$  exceeds  $E_c$ .

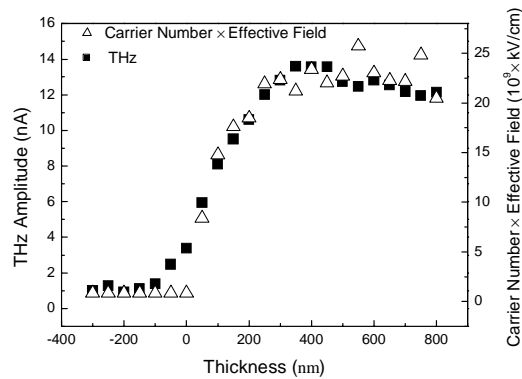


Fig. 6. The product of carrier number and effective electric field,  $n_{ph}E_{eff}$ , and the amplitude of the THz plotted as a function of the intrinsic layer thickness( $d$ ).

### 3. Conclusion

In conclusion, THz radiation from GaAs  $SIN^+$  structures with various surface fields as the bias is studied. The amplitude of the THz radiation peaks at the critical field which depends on the energy difference between the  $\Gamma$  to L valley of the semiconductor. As the field is lower than the critical field, the amplitude is proportional to the product of the surface field and the number of photo-excited carriers. In the high field limit where the surface field exceeds the critical field, the amplitude is independent of the surface field but proportional to the product of the critical field and the number of the photo-excited carriers. The L valley offset can be estimated from THz radiation.